Puzzling magnetic properties of magnetite based glass ceramics

Viorel Sandu[1,*], Mirela Sidonia Nicolescu[1], Simona Greculeasa[1,2], Andrei Kuncser[1,2], Victor Kuncser[1]

[1]*National Institute of Materials Physics, Bucharest Magurele, 077125, Romania*

[2]*Bucharest University, Faculty of Physics, 077125, Bucharest-Magurele, Romania*

(Received 20 July 2015; accepted 21 August 2015)

Structural and magnetic properties of a glass ceramic obtained by crystallization of a glass with nominal composition $26.8B_2O_3$ $6.4Na_2O_3$ $17.5Fe_2O_3$ $47SiO_2$ $0.5Cr_2O_3$ were investigated. High resolution electron microscopy, Mössbauer spectroscopy and magnetization data are consistent with a trimodal size distribution of the crystallites grown in the glassy matrix. One mode corresponds to the submicron, well-structured magnetite crystallites whereas the other two modes correspond to the tiny nanoparticles that are responsible for the low temperature superparamagnetism of the glass ceramic. The relaxation of the magnetization displays a puzzling behavior with an upward relaxation at high temperatures and downward relaxation at low temperatures. An explanation in terms of interplay of the relaxation times is provided.

Keywords: Magnetite; Glass ceramics; Magnetic relaxation; Mössbauer spectroscopy; Superparamagnetism

1. Introduction

Artificial electromagnetic composites have opened a new route for development of microwave communication systems and microwave absorbers. Downsizing of the antennas (e.g., the planar inverted F-antennas) using high permittivity ε_{eff} substrates has a severe impact on the radiation and bandwidth of these devices [1-5]. A solution should be the use of dispersion-free substrates with very large magnetic permeability μ_{eff} comparative to the dielectric constant ε_{eff}, and $\mu_{eff} >> 1$ [6]. They would preserve the radiation quality factor Q unaltered [7]. When the materials of the antenna substrate are composites containing ferromagnetic (ferrimagnetic) inclusions of high magnetic permeability, they can be adjusted to have a matrix with low ε_{eff}. The electromagnetic waves do not probe the fine structural details if their wavelength is large compared to the inclusion size and spacing. For these materials, the complex permeability is close to the static permeability μ_s at frequencies up to the ferromagnetic resonant frequency ω_{res}, which can be considered as the permeability cutoff frequency.

On the other side, the composite materials are extremely competitive for efficient microwave absorbers which are becoming increasingly important for applications such as silent rooms, radar systems, and special military application. An electromagnetic absorber must allow electromagnetic waves to penetrate inside it, where the electromagnetic wave must experience high electric and magnetic losses, within a layer as thin as possible and, obviously, no reflection at the air–absorber interface. In the absorber composite, the ferromagnetic resonance of inclusions, an essential characteristic for enhanced absorption, is determined by a few physical parameters of the magnetic material, namely, anisotropy coefficient K, damping parameter, saturation magnetization M_s, and particle shape. But with particles as small as to display superparamagnetism, the susceptibility and its resonance frequency depend also on the volume of the particles [8]. An important fact is that in a composite with well-dispersed magnetic particles (without percolation), the conductivity is determined mainly by conductivity of the matrix and eddy currents are limited to individual particles. In addition, the shielding and dissipation due to eddy currents rapidly diminish with decreasing particle size.

A reliable candidate for magnetic composites is any magnetite-based glass ceramics (MGC). It consists of magnetite (Fe_3O_4) crystallites grown by glass crystallization in a low permittivity glassy matrix. The method of glass crystallization is very flexible and allows the growth of uniformly distributed magnetic nanoparticles of different shape as a function of glass composition and nucleating agents. Below, we present the structural and magnetic properties of a borosilicate glass ceramics with magnetite crystallites. Some of these properties show abnormal strange features.

2. Experimental details

The magnetic glass-ceramic sample was fabricated by crystallization of a borosilicate glass melt with the nominal composition $26.8B_2O_3$ $6.4Na_2O_3$ $17.5Fe_2O_3$ $47SiO_2$ $0.5Cr_2O_3$, where Cr_2O_3 plays the role of nucleating agent. The ingredients, SiO_2, H_3BO_3, Na_2CO_3, Fe_2O_3, and Cr_2O_3 were thoroughly mixed and the batch was melt at 1430°C for 3 h. Then, the sample

was cast onto a preheated steel mould. The resulting glass slab was thermally treated at 560°C for two hours and, finally, the samples were cooled dawn to room temperature.

Structural and compositional investigations were performed by X-ray diffraction (Bruker-AXS-D8 Advance diffractometer with Cu K radiation), electron microscopy (JEM 200CX TEM/SCAN and JEM-ARM200F), and Mössbauer experiments. The magnetic properties were investigated with an MPMS SQUID magnetometer (Quantum Design) in the temperature range 5-300 K.

3. Results and discussion

3.1 Structure and morphology

Fig. 1 shows the phase structure of the sample, as resulted from XRD data. Magnetite is well crystallized and is the dominant crystalline phase detected in all samples but traces of hematite (α -Fe2O3) are also visible. The degree of crystallinity is 52.4% whereas the crystallite size as obtained from the half width of the diffraction peaks is 121 nm. However, as high resolution transmission microscopy and Mössbauer data show, the size structure is more complex.

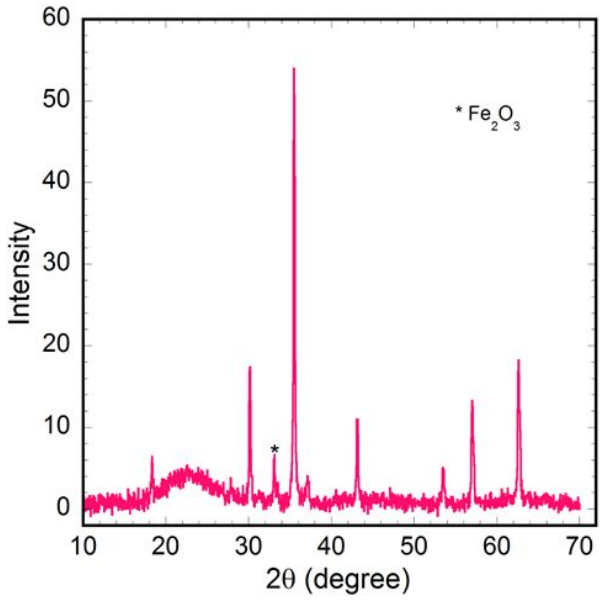

Fig. 1 X-ray diffraction graph of the magnetite-based glass ceramic obtained from crystallization of Fe containing borosilicate glass melt. Both the background and $K\alpha_2$ contributions were subtracted.

The microscopy data show a multiple modal size distribution of the crystallites with large cubic crystallites of about 80-130 nm (Fig. 2.a) embedded in a "sea" of tiny but uniformly distributed nanoentities of 3-10 nm (Fig. 2.b), as high resolution transmission electron microscopy (HRTEM) shows. Most probably, that multimodal distribution is the result of two ways of crystallization, one generated by nucleating agents (the large crystallites) and the tiny ones of athermal origin. The smaller crystallites were also identified as magnetite by electron diffraction and STM-EELS spectra. A careful investigation shows that the tiny nanocrystals have a bimodal size distribution, a feature which was also revealed by neutron diffraction in other magnetite-based glass ceramics [9].

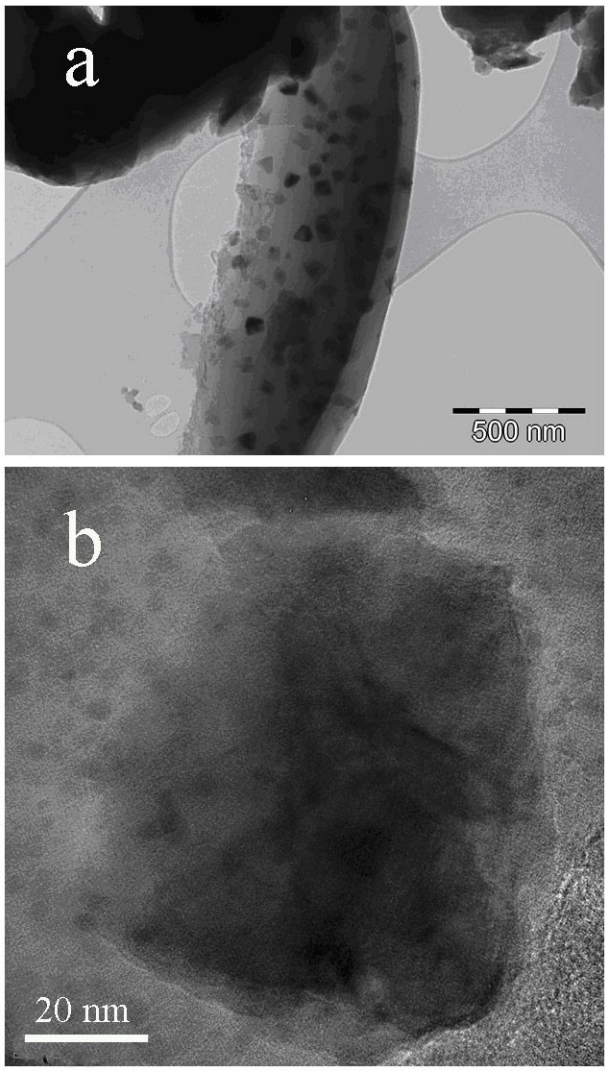

Fig. 2 TEM micrograph of the magnetite-based glass ceramic obtained by crystallization of Fe-containing borosilicate glass melt.

3.2 Mössbauer spectroscopy

Ideal magnetite has an inverse spinel structure $Fe^{3+}[Fe^{3+}Fe^{2+}]O_4$ where the first Fe^{3+} ions occupy the tetrahedral sites whereas the octahedral sites are filled by an equal mix of Fe^{3+} and Fe^{2+} ions. At high temperatures, an electron from the two types of Fe ions on octahedral positions is delocalized and, consequently, may be treated as resonating on the octahedral position, with a corresponding mean valance of +2.5 on this positions. According to that

structure, the ratio of the occupied sites with Fe ions in the octahedral and tetrahedral positions is $R_0 = 2$ in ideal magnetite. Any change of this value indicates a deficiency of Fe ions in one of the two sublattices. Due to the resonant electron, at temperatures above the Verwey temperature T_V, the Mössbauer data are usually fitted only with four sublattices, two sextets depicting the magnetic contribution corresponding to the two position (tetrahedral and octahedral) and two doublets corresponding to the paramagnetic ions. The ratio of the relative spectral areas corresponding to the two sextets is proportional to the ratio of octahedral/tetrahedral site occupation R. At low temperatures, $T < T_V$, where the common electron is frozen, the Mössbauer data were fitted by six sublattices (see Fig. 3). Four out of the six sublattices were attributed to magnetic contributions (sextets) belonging to Fe^{3+} and Fe^{2+} positions in both octahedral and tetrahedral positions and the two others (doublets) to paramagnetic Fe ions. The transition temperature between the two configurations should be considered as related to the Verwey transition.

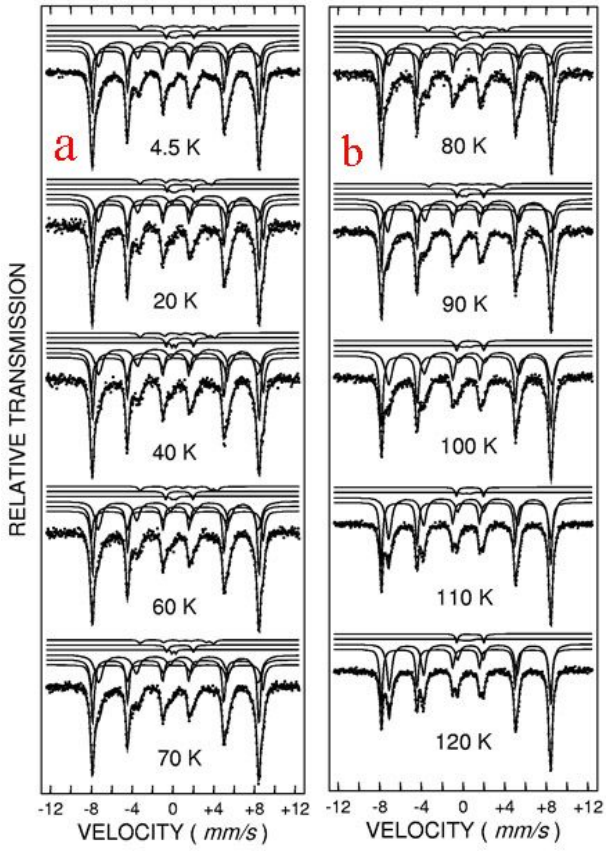

Fig. 3 Mössbauer spectra of the magnetite-based glass ceramic, collected at different temperatures a) 5 – 70 K and b) 80 – 120 K

The additional two paramagnetic spectral components at low temperatures were attributed to Fe^{2+} and Fe^{3+} ions, respectively, and originate both in the Fe ions which still participates to the glassy network and to the superparamagnetic tiny nanoparticles.

As Fig. 3 shows, T_V must be located between 90 and 100 K. The Fe^{3+} superparamagnetic component is roughly negligible whereas the relative area of Fe^{2+} superparamagnetic component is higher than 10% in most spectra. The temperature dependence of the relative area of the central doublets shows a significant increase of the paramagnetic spectral contributions just below 40 K (Fig. 4).

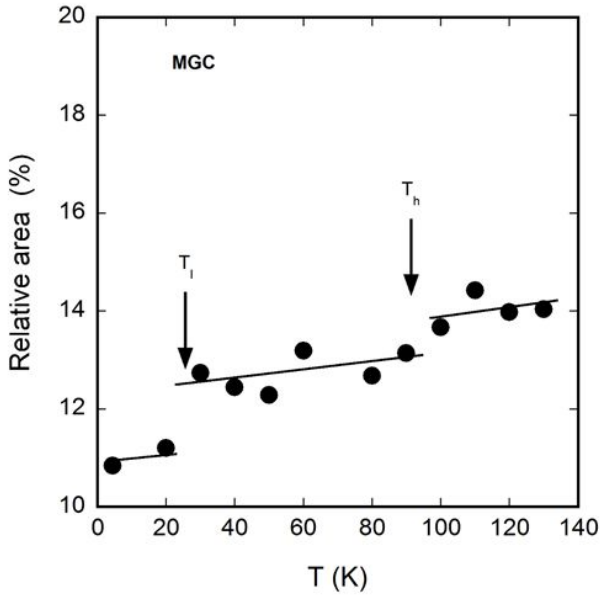

Fig. 4 Temperature dependence of the total relative area of the central doublets for the magnetite containing glass ceramics in Verwey state.

The increase was attributed to the superparamagnetic (SPM) transition of the tiniest crystallites that, obviously, have a low blocking temperature [10]. A second increase is noticeable above 90 K. That suggests the existence of a second upper blocking temperature. We mention that the large crystals might have the blocking temperature above the room temperature, hence, they are completely blocked in the temperature range of our investigation. Therefore, the existence of two blocking temperatures below 100 K mirrors the bimodal distribution of the tiny nanoparticles, namely, one mode with a size average of about 5 nm and one mode with a size average about 8 nm. These tiny nanoparticles do not display a Verwey transition, which has a structural origin, but can generate SPM blocking. Data at room temperature are consistent with an occupation ratio $R =$

2.1 which is close to R_0.

3.3 Magnetic properties

Magnetization M vs temperature T data mirror the complex physics of a system consisting of several magnetic nanoentities in a paramagnetic matrix, which also involves magnetically active grain surfaces. It is noteworthy that Verwey state itself has a complex physics with many aspects still under debate [11, 12]. The large magnetite crystallites impose those features which are specific to magnetite (Verwey transition and Curie temperature) whereas the small magnetite nanoparticles generate the low temperature SPM behavior. As Mössbauer and HRTEM data suggest, the small nanoparticles have a bimodal size distribution which is consistent with the existence of two blocking temperatures. However, the temperature dependence of the magnetization, Fig. 5, clearly shows only the low blocking temperature T_l = 46.5 K (which corresponds to the nanoparticles of 5 nm average size) while the higher blocking temperature, T_h = 96 K, could be identified only on the derivative of the zero field cooled (ZFC) magnetization probably because of the larger dispersion of the high temperature mode.

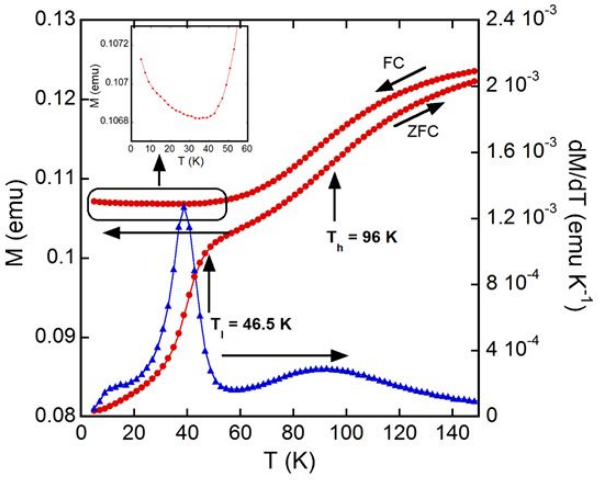

Fig. 5 Temperature dependence of magnetization of MGC (left axis) and the temperature derivative of the magnetization (right) as measured at 25 Oe. Inset: zoom of the low temperature range of FC branch.

The presence of a deep in the FC curve as well as the increase of magnetization at very low temperatures (see the inset to the Fig. 5) but also the absence of aging effects suggest a mixture of SPM, which is dominant, and superspin glass (SSG) state. The latter contribution originates in the magnetically disordered layer that is present at the surface of the nanoparticles [13].

The time t evolution of the remanent magnetization, which was measured after the field was ramped up to 2 T, held for 60 seconds at this value and, finally, removed to zero, is shown in Fig. 6 for different temperatures. Usually, in ordinary magnetic systems, remanent magnetization decays in time (downward relaxation). What is puzzling, the remanent magnetization decreases only below T_l but it shows an increase in time (upward relaxation) when it occurs at higher temperatures but below T_h.

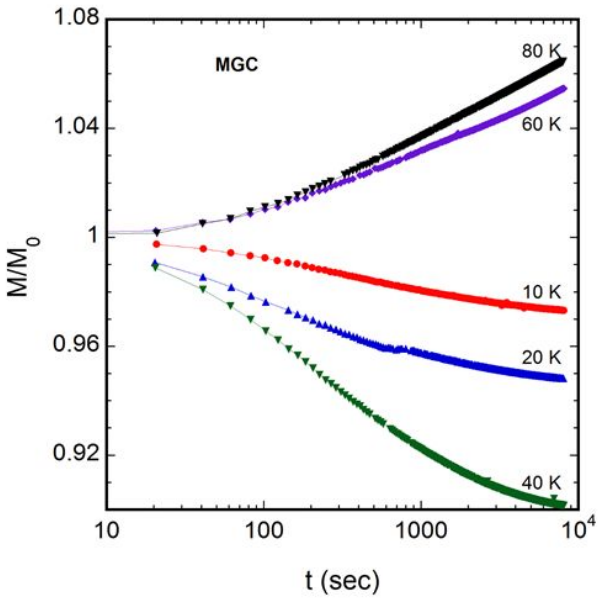

Fig. 6 Time dependence of the remanent magnetization normalized to M_0=M(t=0) for magnetite-based glass ceramic.

4. Discussion

The increase of the magnetization is hard to understand in the framework of the theories describing the relaxation of magnetization in magnetic systems. Moreover, it is hard to understand why the relaxation rate, defined as, changes the sign in narrow temperature ranges and why the negative (upward) relaxation occurs at higher temperatures while normal, positive relaxation takes place at lower temperatures. Actually, upward relaxation means that an external magnetic field drives the sample in a magnetic state with a magnetic ordering displaying a smaller magnetization than in the absence of the field. The system slowly recovers the original ordering with high magnetization state only after the field is switched off. Obviously, the changes in the magnetic ordering must be related to the actual spin structure of the nanoparticles. It is now accepted that magnetic nanoparticles consist of a magnetically ordered core and a magnetically disordered outer layer [13]. This outer layer, the shell, might be the clue in the

relaxation process. The orientation of the outer, disordered spins and even the magnetic ordering can be easily controlled by an applied field. However, it relaxes back when the field is suppressed. In addition, these nanoparticles relax also by superspin reversal (Néel relaxation), which is fast at temperatures above blocking temperature, but dramatically slows down below the blocking temperatures. Thus, the relaxation must be the result of the interplay between the two mechanisms of relaxation. Specifically, at temperatures higher than the blocking temperatures, the Néel relaxation (spin reversal) occurs fast, hence, the relaxation of the shell spins prevails, while below the blocking temperature, the superspin reversal needs longer times, hence, it starts to dominate. Spin reversal always leads to lower magnetization as it depicts the tendency to equal the density of the superspins in the up and down states. Consequently, at temperatures below $T_l \approx 46$ K, all nanoparticles are in a blocked SPM state regardless the mode of the distribution size. Therefore, the relaxation is controlled by the spin reversal, which is slow. Above this temperature, only a fraction of the nanoparticles remain blocked, namely, the larger nanoparticles, 8-10 nm, with blocking temperatures at $T_h > T_l$. Thus, the dominant mechanism for relaxation at $T_l < T < T_h$ might be controlled by the shell spins of the tiniest nanoparticles. In order to explain their upward relaxation, Lin He [14] has conjectured that the applied field tunes the interaction between the core spins and the spin glass shell into an antiferromagnetic coupling at temperatures above the freezing temperature of the disordered spins. Thus, the total magnetization in the presence of the field would be $m(\mathrm{H}, \mathrm{T}) = m_{core}(\mathrm{H}, \mathrm{T}) - m_{sg}(\mathrm{H}, \mathrm{T})$ where m_{sg} is the net magnetization of core spins that antiferromagnetically couple to the shell. After the magnetic field is removed, the AF interaction vanishes and the remnant magnetization starts to increase toward m_{core}.

5. Conclusion

We have investigated the magnetic properties of a glass ceramic obtained by crystallization of a glass with nominal composition $26.8B_2O_3$ $6.4Na_2O_3$ $17.5Fe_2O_3$ $47SiO_2$ $0.5Cr_2O_3$. The magnetite which grows in the glassy matrix displays a trimodal size distribution with one mode corresponding to large, submicron sized, magnetite crystals and two other modes corresponding to the tiny nanometric nanoparticles with average size at 5 nm and 8 nm, respectively. The large particles are responsible for the magnetite like features of the glass ceramic whereas the tiny nanoparticles provide characteristics typical for superparamagnetic systems which include the existence of two blocking temperatures corresponding to the two modes of the size distribution. It is to mention that the blocking temperature of the large particles must be of order of their Curie temperature, $T_C \approx 850$ K hence, above the room temperature.

The puzzling behavior of the relaxation of the magnetization, which changes the sign of the relaxation rate from upward relaxation to downward relaxation as the temperature is decreased below 46 K, is explained by two facts: i) the existence of a magnetically disordered shell which might be antiferromagnetically ordered by an external field; and ii) the interplay between the relaxation times by spin reversal and by shell spins disordering. At temperatures below the lower blocking temperatures, the slow relaxation by spin reversal dominates whereas at higher temperatures dominates the relaxation is controlled by shell spins order-disorder process.

Acknowledgment

This work was supported by the Romanian Ministry of Education, Executive Unit for Funding High Education, Research, Development and Innovation under the Idea-Complex Research Grant PN-II-ID-PCCE-2011-2-0006 (contract #3/2012) and Core Program PN 45N.

References

[1] I. J. Bahl, P. Bhartia, Microstrip Antennas, Artech House, Massachusettes, 1980.

[2] K. R. Carver, J. W. Mink, *IEEE T. Antenn. Propag.*, 29 (1981) 2

[3] C. A. Balanis, Antenna Theory: Analysis and Design. John Wiley & Sons, New York, 1997

[4] R. K. Mongia, A. Ittipiboon, M. Cuhaci, *Electron Lett.*, 30 (1994) 1362

[5] J. S. Colburn, Y. Rahmat-Samii, *IEEE T. Antenn. Propag.*, 47 (1999) 1785

[6] R. C. Hansen, M. Burke, *Microw. Opt. Techn. Let.*, 26 (2000) 75

[7] O. Edvardsson, Proc. ICAP Int. Conf. Antennas Propag., Manchester, UK, Apr. 17–20, 2001, 17

[8] J. L. Dormann, D. Fiorani, E. Tronc, *Adv. Chem. Phys.*, 98 (1997) 283

[9] U. Lembke, A. Hoell, R. Kranold, R. Müller, W. Schüppel, G. Goerigk, R. Gilles, A. Wiedenmann, *J. Appl. Phys.*, 85 (1999) 2279

[10] G. Schinteie, V. Kuncser, P. Palade, F. Dumitrache, R. Alexandrescu, I. Morjan, G. Filoti, *J. Alloy. Compd.*, 564 (2013) 27

[11] J. García, G. J. Subías, *J. Phys.-Condens. Mat.*, 16 (2004) R145

[12] A. Tanaka, C. F. Chang, M. Buchholz, C. Trabant, E. Schierle, J. Schlappa, D. Schmitz, H. Ott, P. Metcalf, L.H. Tjeng, C. Schußler-Langeheine, *Phys. Rev. B*, 88 (2013) 195110

[13] J. M. D. Coey, *Phys. Rev. Lett.*, 27 (1971) 1140

[14] L. He, *J. Appl. Phys.*, 109 (2011) 123915

* To whom correspondence should be addressed. Email: vsandu@infim.ro